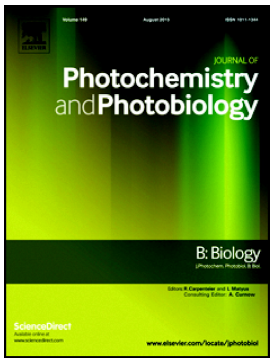

Verteporfin-loaded mesoporous silica nanoparticles inhibit mouse melanoma proliferation in vitro and in vivo

Nausicaa Clemente, Ivana Miletto, Enrica Gianotti, Marco Invernizzi, Leonardo Marchese, Umberto Dianzani, Filippo Renò

PII: S1011-1344(19)30111-3
DOI: https://doi.org/10.1016/j.jphotobiol.2019.111533
Article Number: 111533
Reference: JPB 111533

To appear in: *Journal of Photochemistry & Photobiology, B: Biology*

Received date: 25 April 2019
Revised date: 7 June 2019
Accepted date: 12 June 2019" role="suppressed

Please cite this article as: N. Clemente, I. Miletto, E. Gianotti, et al., Verteporfin-loaded mesoporous silica nanoparticles inhibit mouse melanoma proliferation in vitro and in vivo, Journal of Photochemistry & Photobiology, B: Biology, https://doi.org/10.1016/j.jphotobiol.2019.111533

Verteporfin-loaded mesoporous silica nanoparticles inhibit mouse melanoma proliferation in vitro and in vivo

Nausicaa Clemente[a], Ivana Miletto[b], Enrica Gianotti[b], Marco Invernizzi[c], Leonardo Marchese[b], Umberto Dianzani[a], Filippo Renò[c,*] filippo.reno@med.uniupo.it

[a]Department of Health Sciences and Interdisciplinary Research Center of Autoimmune Diseases (IRCAD), University of Eastern Piedmont, via Solaroli, 17 – 28100, Novara, Italy.

[b]Department of Science and Technological Innovation and Nano-Systems Center, University of Eastern Piedmont, Viale T. Michel, 11 - 15121 Alessandria (AL), Italy.

[c]Department of Health Sciences and Innovative Research Laboratory for Wound Healing, University of Eastern Piedmont, via Solaroli, 17 – 28100, Novara, Italy.

[*]Corresponding author at: Department of Health Sciences and Innovative Research Laboratory for Wound Healing, University of Eastern Piedmont, via Solaroli, 17 – 28100, Novara (NO), Italy.

Abstract

Melanoma is one of the most lethal tumors among the skin cancers, arising from complex genetic mutations in melanocyte. Melanoma microenvironment is very heterogeneous, showing complex vascular networks and immunogenicity, as well as induced acquired resistance to treatments by upregulation of multidrug resistance (MDR) mechanisms. Different studies have showed that Photodynamic Therapy (PDT) could be considered a new potential approach for melanoma treatment. PDT combines a light with a specific wavelength and a photosensitizer: when these two elements interact reactive oxygen species (ROS) are generated leading to tumor cell destruction. In this study verteporfin (Ver), a second-generation photosensitizer, has been conjugated with mesoporous silica nanoparticles (MSNs): the resulting Ver-MSNs are an efficient nanoplatforms used to enhance cargo capacity and cellular uptake. Our in vitro and in vivo studies investigated whether Ver-MSNs were able to reduce or inhibit melanoma growth. In vitro experiments performed using B16F10 mouse melanoma cells showed that Ver-MSNs stimulated by red light (693nm) significantly decreased in vitro cells proliferation in a range of concentration between 0.1 µg/ml to 10 µg/ml. When Ver-MSNs (5 µg/ml in glycerol) were topically administrated to melanoma tumor mass developed in mice and stimulated by red light for four times in 16 days,

they were able to reduce the tumor mass of 50.2 ±6,6 % compared to the untreated (only glycerol) mice. In the light of this information, PDT performed using Ver-MSNs could be considered a new promising and potential approach to treat melanoma.

Keywords: Melanoma; Photodynamic therapy; Verteporfin; Mesoporous silica nanoparticles; B16F10 cells; ROS.

1. Introduction

Melanoma is one of the most aggressive and dangerous form of skin cancers [1,2]. The World Health Organization (WHO) stated the worldwide number of people diagnosed is growing faster than any other tumors. Moreover, according to the epidemiological studies, its incidence will be double in the next 10-20 years, becoming a significant and concrete concern of public health all over the world [3,4]. Malignant melanoma is known to be particularly difficult to treat because of its high resistance to the currently available treatments such as radiotherapy and chemotherapy. Nowadays, the only option to excise the tumor is surgery [4,5].

Recently FDA (Food and Drug Administration) has approved a new promising method called Photodynamic therapy (PDT). This approach has already been used in treating various pathologies such as actinic keratosis, ophthalmologic diseases and other types of cancer as non-small cell lung cancer [6–8].

PDT combines a photosensitizer, administrated or applied locally to the target, and a light of a specific wavelength able to penetrate tissues. When the photosensitizer is irradiated by proper light, it generates reactive oxygen species (ROS) [9,10]. These resulting products of the interaction between the photosensitizer and light, kill malignant cells, cause destruction of the vascular structure and lead to the inflammatory response activation [11–13].

A photosensitizer largely employed in PTD is Verteporfin, a benzoporphyrin derivative, [14,15] which is a second-generation photosensitizer approved by the Food and Drug Administration (FDA) for the treatment of age-related macular degeneration [4,6,14]. Ver is characterized by an intense absorption band in the red region of the visible spectrum and red light has proved ability to penetrate tissue in a deeper way than the other visible wavelengths [14].

To avoid the event of aggregation in aqueous media because of its hydrophobicity, Ver was strategically conjugated with mesoporous silica nanoparticles (MSNs) [4].

Due to their intrinsic structural properties such as large surface area, high pore volume, uniform pore size and easy chemical functionalization, MSNs have been extensively investigated as nanocarriers for drugs in nanomedicine [14–16] and specifically in PTD applications [17].

.

The resulting Ver-MSNs obtained by covalent conjugation of amino-functionalized mesoporous silica nanoparticles (NH2- MSNs) with verteporfin (Ver) was a highly efficient nanoplatform for PDT [4,14].

The purpose of our in vitro and in vivo study was to evaluate the efficacy of photodynamic therapy with verteporfin-loaded mesoporous silica nanoparticles as a possible treatment for skin melanoma.

2. Materials and methods

2.1 *Synthesis of Ver-MSNs*

Verteporfin-loaded mesoporous silica nanoparticles were prepared according to literature procedures [4,15].

MSNs nanoparticles were synthesized using cetyltrimethylammonium bromide (CTAB) (Sigma-Aldrich) as structure directing agents and tetraethylorthosilicate (TEOS) (Sigma-Aldrich) as the silica source. CTAB was dissolved in distilled water and NaOH. Later, TEOS was added dropwise under vigorous stirring. The resulting mixture was stirred at 80°C for 2 h.

After stirring, a white precipitate was formed. It was filtered off and washed, then the CTAB surfactant was removed from the as-prepared material through calcination.

The ensuing dried MSNs were used to prepare aminopropyl-functionalized mesoporous nanoparticles (amino-MSNs). To this purpose, MSNs were suspended in toluene, aminopropyltriethoxysilane (APTES) (Sigma-Aldrich) was added dropwise and the mixture was stirred under reflux overnight. The obtained white solid was recovered by filtration, washed with ethanol and deionized water and dried in oven.

Amino-MSNs suspended in dimethylformamide (DMF) (Sigma-Aldrich) were enriched with a DMF solution (10 mL) containing Verteporfin (Ver) (Sigma-Aldrich), 1-[Bis(dimethylamine)methylene]-1H-1,2,3-triazolo[4,5-b] pyridinium3-oxide- hexafluoro-phosphate (HATU, 1 eq.) (Sigma-Aldrich) and N,N-diisopropylethylamine (DIPEA, 1 eq.) (Sigma-Aldrich) to form Ver based silica nanoparticles.

After a 24-hour stir, the solid was filtered and then dried under vacuum. Ver containing amino-MSNs material (Ver-MSNs) was prepared with a nominal Ver loading of 40 mg/g; this loading value was chosen on the basis of previous work [14].

The Ver-MSNs solid was washed several times with DMF to remove the unreacted Ver molecules. The actual Ver loading was calculated from the UV-Vis spectra of the Ver eluate after the washing procedure, using the Lambert-Beer law (ε = 35000 M^{-1} cm^{-1} in DMF): the average number calculated of Verteporfin per MSNs was about 4.3 x 10^4.

The synthetic procedure of the preparation of Ver-MSNS is shown in Figure 1.

2.2 *Characterization of Ver-MSNs*

Fourier Transform Infrared Spectroscopy (FTIR) was used to confirm the covalent coupling between Verteporfin and NH_2-MSNs [4,14]. X- ray diffraction (XRD) and High-resolution transmission electron microscopy (HRTEM) were performed to examine whether the introduction of verteporfin inside the mesoporous silica nanoparticles had modified the structure and dimensions of MSNs. The results showed that the verteporfin conjugation did not affect the typical pattern of an ordered hexagonal network of MSNs [4,14].

2.4 *Indirect determination of Singlet oxygen*

Uric acid (UA) (Sigma-Aldrich) was used as a scavenger molecule to evaluate the release of singlet oxygen to the solution by the Ver-MSNs nanoparticles in aqueous media (pH 7.0). [4,18] The experiment was carried out by irradiating the sample with a light source at 690 nm (450 W Xenon lamp); after fixed time intervals, absorption spectra were collected on a Perkin Elmer Lambda 900 spectrometer. The $^1O_2$ scavenger absorption was monitored through a decrease in the electronic absorption band of UA at 292 nm and the normalized UA absorption at 292 nm was plotted as a function of the irradiation time.

2.5 Cell culture

B16-F10 cells were grown in RPMI medium (Carlo Erba, Milan, Italy) supplemented with 10% heat inactivated fetal bovine serum (FBS) (Carlo Erba), penicillin (100 U/mL), streptomycin (100 mg/L) and L-glutamine (2 mM) (Carlo Erba) in a humidified atmosphere containing 5% CO_2 at 37°C [4].

2.6 *Cell treatment*

Confluent cells were trypsinized, counted and 1 x 10^4 cells/well were seeded in a 48 multiwell culture plate and allowed to adhere overnight. Non adherent cells were removed by gentle wash in phosphate buffered saline solution (PBS, pH = 7.4) before nanoparticle incubation.

Cells were incubated for 4 hours with silica nanoparticles (MSNs), silica nanoparticles loaded with 4% verteporfin (Ver-MSNs) both at 0.1, 0.5, 1, 5, 10 µg/ml concentration or with cell culture medium alone as control. Nanoparticles were resuspended in RPMI without phenol red and without FBS. [4]

At the end of the incubation culture medium with or without silica nanoparticles was removed and the cells were irradiated with a 650/8 filter for 180 sec with a plate reader (Victor X4, Perkin-Elmer, Waltham, MA, USA) or leaved without irradiation (in dark condition). After irradiation, new complete culture medium was added to each well and cells were let to grow overnight, also in dark condition was changed the medium. At the end of treatments MTT assay was performed.

2.7 *MTT assay*

Cell proliferation was evaluated by MTT assay, an experimental approach based on tetrazolium salts reduction [19,20]. 5x10^3 cells/well were seeded in a 96 wells cell culture plate and allowed to adhere overnight before experimental treatment. Cells were incubated in the different conditions of interest for 48 h. At the end of the incubation time, cells were incubated in cell culture medium without phenol red (Euroclone, Milan, Italy) containing 0.5 mg/ml MTT (Thermo Fisher Scientific, Waltham, MA, USA) for 4h at 37°C to allow formazan salts precipitation. The resulting insoluble purple precipitate was then dissolved in DMSO (Carlo Erba Reagents, Cornaredo, Italy) and the absorbance was read at 570 nm using a microplate reader (Victor X4, Perkin-Elmer, Waltham, MA, USA).

2.8 *Animal studies*

Female 8-wk-old C57BL6/J (The Jackson Laboratory, Bar Harbor, ME) mice were bred under pathogen-free conditions in the animal facility of the University of Eastern Piedmont and treated in accordance with the University Ethical Committee and European guidelines. The mice were injected subcutaneously with B16-F10 cells ($2.5x10^5$ in 100 µl /mouse) and the tumour growth was monitored every four days. Eleven days after the tumour induction, when the tumour was palpable, mice were treated via transcutaneous administration of 2 ml of solution of MSNs (5 µg/ml) in glycerol, Ver-MSNs (5 µg/ml) in glycerol or the same volume of glycerol as negative control. Five minutes after each transcutaneous administration, mice were exposed to red light for ten minutes. The treatment had been carried out four times every four days and the mice were sacrificed four days after the last administration, or when they displayed sufferance. Five animals for groups were employed for each group.

2.9 *Histology and immunofluorescence on tumours*

After euthanasia, all animals underwent complete necropsy to evaluate macroscopic alterations. Tumour samples were embedded in optimal cutting temperature (OCT) compound (Bioptica Milano SpA, Italia), snap-frozen, and stored at -80 °C until use. Tumour tissues were cut with a cryostat (thickness 5-6 µm) and treated with 4% paraformaldehyde (Sigma-Aldrich) diluted in PBS for 5 minutes at room temperature to fix the sample on the glass slides. The samples were then blocked with 5% Normal Goat Serum (R&D System, Minneapolis, USA) in PBS for one hour, to block aspecific sites. To detect CD31 expression, slides were incubated with the primary polyclonal antibody anti-CD31 (1:50, Abcam, Cambridge, UK) overnight 4°C. The antibody was detected using an anti-rabbit Ig Alexa fluor 488-conjugated (1:400, Thermo Fisher).

Then, the sections were stained with 0.5 mg/ml of the fluorescent dye 4,6-diamidino-2-phenylindole-dihydrochloride (DAPI, Sigma-Aldrich) for 5 minutes, to color the cell nuclei, and then mounted using Prolong anti-fade mounting medium (Slow Fade AntiFADE Kit, Molecular Probes Invitrogen). The complete procedure was performed in a humidified chamber. The sections were then observed by a fluorescence microscope (Leica, Italy), and analyzed with the Image Pro Plus Software for micro-imaging 5.0 (Media Cybernetics, version 5.0, Bethesda, MD, USA). Sections of tumours were also stained with Hematoxylin and Eosin (H&E).

2.10 **Statistical analysis**

ANOVA test followed by Bonferroni's post test was used for statistical analysis. Statistical procedures were performed with the GraphPad Instat statistical software (GraphPad Software Inc., CA, USA). Probability values of $p < 0.05$ were considered statistically significant.

3. **Results**

Ver-MSNs are photosensitizer based nanodevices which generate ROS such as singlet oxygen, hydrogen peroxide and hydroxyl radical, under light exposure [21,22]. Ver-MSNs were obtained by covalent anchoring of Ver to amino-modified MSN, through the formation of amide bond. The successful anchoring of Ver was assessed by infrared spectroscopy[14]. In figure 2 the FTIR spectra of Ver, MSNs and Ver-MSNs are reported. In the high frequency range, the FTIR spectrum of MSNs (red curve) shows signals at 2967, 2930 and 2870 cm^{-1} due to asymmetric and symmetric stretching modes of C-H bond in CH_2 groups of the aminopropyl chain and in CH_3 groups of uncondensed ethoxy groups of 3-aminopropyltriethoxysilane. The bending modes of methylene groups can be found in the low frequency range, between 1500 and 1350 cm^{-1}, whilst the bending mode of NH_2 groups is responsible for the signal at ca. 1630 cm^{-1}. The high frequency region of FTIR spectrum of Ver (black curve) is characterized by signals arising by methyl and methylene groups stretching vibrations (2700-3000 cm^{-1}) and by the stretching modes of N-H (3300-3400 cm^{-1}) group of the porfin ring and of the O-H group of terminal carboxylic acid of Ver (ca. 3530 cm^{-1}). In the low frequency region, the spectrum is dominated by the intense signal at 1700 cm^{-1}, due to C=O stretching vibration. Signals below 1500 cm^{-1} are ascribed to the bending vibrations of methyl and methylene groups. Last, the FTIR spectrum of Ver-MSNs (green curve) is characterized by similar CH stretching signals in the high frequency region, coming both from the amino-modified support and from the Ver molecule; in the low frequency region the presence of the band at 1660 cm^{-1} and 1595 cm^{-1} due to the C=O stretching and N-H bending modes of the amide group give confirmation of the covalent anchoring of Ver molecules through amide bond.

The release of singlet oxygen ($^1O_2$) in solution was evaluated by a chemical indirect method which employs uric acid (UA), a scavenger molecule which undergoes oxidation during the illumination of verteporfin [15,23–26].

The production of oxidized substrate was determined by the consumption of singlet oxygen: the UA concentration decrease is directly related to the quantity of $^1O_2$ [24]. At neutral pH, uric acid is stable as a monoanion with a band at 292 nm [15]. When singlet oxygen is produced, as a result of Ver- MSNs irradiation by a light source at 690 nm, uric acid is irreversibly oxidized and a decay of UA band can be observed. Instead, plain MSNs irradiated by the same light source, did not generate singlet oxygen and uric acid is not oxidized. Figure 3 reported the decay curves of uric acid absorption at 292 nm monitored by UV-Vis spectroscopy for 80 min as a function of the irradiation time. The Ver-MSNs decrease is compared to the plain MSNs decay: in presence of verteporfin, uric acid band decreased due to singlet oxygen production, whereas without the photosensitizer, UA band is not modified [4,14-15]. The efficiency of singlet oxygen delivery of Ver-MSNs was calculated using the equation 1 [14,15],

$$\eta_{(Ver-MSNs)} = \Phi_{Ver}\,{}^{1}O_{2}\,\frac{t_{Ver}}{t_{(Ver-MSNs)}}$$

where Φ_{Ver} is the efficiency of Ver in methanol solution (Φ_{Ver}=0.76), t_{Ver} is the UA decreasing time in the presence of Ver in methanol solution and $t_{Ver\text{-}MSN}$ is the UA decreasing time in the presence of Ver-MSNs in water suspension, both times adjusted to a first-order exponential decay. The obtained value for Ver-MSNs singlet oxygen release efficiency was $\eta_{Ver\text{-}MSNs}$=0.30. [14]

As the irradiated Ver-MSNs released singlet oxygen [21,22], the verteporfin loaded silica nanoparticles were tested in vitro as a possible tool for PDT and their effects on cell proliferation and survival in absence or presence of red light in a B16-F10 mouse melanoma cellular model were measured. B16-F10 cells were incubated for 4 hours in the presence of various concentrations of Verteporfin-loaded mesoporous silica nanoparticles both with and without red light stimulation and cell toxicity was evaluated by MTT assay [4]. As shown in figure 4, Ver-MSNs decreased cell survival in both darkness and, at higher levels, under light exposure. In darkness, the effect of Ver-MSNs was detected starting from the 1 μg/ml concentration, where cell viability was 61,89% (0,177 ± 0.01 SD) of that detected in the samples treated with MSNs in darkness, and it did not increase at higher drug concentrations. Upon exposure to red light, the Ver-MSNs effect was already detectable at the 0.1 μg/ml concentration (cell viability: 68,26% (0,157 ± 0,008 SD), $p<0.001$ compared to red light irradiated plain MSNs) and it increase in a concentration dependent manner reaching a maximum level of 67,39% (0,075 ± 0.022 SD) when treated with 10 μg/ml.

To evaluate the efficacy of Ver-MSNs as a possible photodynamic therapy for melanoma in vivo, female mice were injected subcutaneously with B16-F10. Eleven days later, when tumours were

palpable, mice were treated transcutaneously with glycerol, MSNs and Ver-MSNs and then irradiated with a red light. Treatment was repeated four times every four days. The tumour volume was evaluated every four days with a caliper and the tumour weigh was evaluated at the endpoint. Figure 5a shows the kinetics of tumour growth in terms of volumes and shows that mice treated with Ver-MSNs displayed significantly lower tumor growth than those treated with either glycerol or MSNs. Moreover, treatment with MSNs alone was per se able to inhibit the tumour growth compared to that with glycerol. Analysis of the tumour weight at the end-point confirmed that treatment with Ver-MSNs significantly inhibited tumour growth compared to treatment with MSNs alone or glycerol, and that treatment with MSNs alone was per se able to inhibit the tumour growth compared to that with glycerol. Four days later the last administration or when they displayed sufferance, the mice were sacrificed and tumours were removed and weighted. Tumour weight of mice treated with MSNs and Ver-MSNs was significantly reduced compared to the one of untreated mice (figure 5b). This reduction suggests that mesoporous silica nanoparticles under red light are able to inhibit tumour growth. In particular, the regression of tumour weight is more important in mice treated with Ver-MSNs meaning that verteporfin is implied in the inhibition of tumour.

Tumor angiogenesis was evaluated by staining CD31, marking vascular endothelial cells, in the tumor sections [27]. Results showed a significant reduction of vessels in the tumors from mice treated with Ver-MSNs compared to those from mice treated with either MSNs or glycerol. By contrast, vessels were not reduced, but rather increased, in the tumor from the mice treated with MSNs compared to those from the mice treated with glycerol (figure 6a, 6b).

4. Discussion

Malignant melanoma is one of the most dangerous and deadliest skin tumors causing the majority of death among all the skin cancers [28,29]. Moreover its incidence rate increases every year of about 3 per cent [30,31].

Because of its high resistance to radiotherapy and chemotherapy and its ability to progress silently remaining invisible, international studies focus on innovative potential treatment tools [4,5,32,33] like photodynamic therapy (PDT). It is a minimally invasive, local application approved by Food and

drug administration already used in medicine for ophthalmological diseases as age related macular degenerations, actinic keratosis and other forms of cancers [6,13,34,35].

This new strategy needs three indispensable elements: a photosensitizer, molecular oxygen and a specific wavelength of light [33]. Initially, the photosensitizer is irradiated by a specific wavelength becoming active and able to react with molecular oxygen [36]. The generation of reactive oxygen species ROS is able to damage cancer cells, block the arrival of oxygen and essential nutrients to blood vessels and activate the inflammatory and immune responses [11,37,38].

A FDA approved photosensitizer in PDT is Verteporfin, a benzoporphyrin derivative monoacid ring A (BMP-MA); it's commercial formulation is Visudyne® [39].

However, due to its hydrophobic structure, Verteporfin tends to aggregate in aqueous solutions [4]. In order to avoid aggregation, to improve cellular uptake, to protect loaded molecules from photobleaching and to load a high cargo, Verteporfin was successfully grafted on mesoporous silica nanoparticles (MSNs). MSNs are a biocompatible platform for drug delivery already used in medicine [4,15] and more recently in PDT [17].

In consideration of these notions, we conjugated MSNs with verteporfin and tested the resulting nanocarrier as a possible strategy to treat melanoma by performing in vitro and in vivo experiments [4]. The in vitro experiments showed that growth of B16-F10 melanoma cells was significantly inhibited by Ver-MSNs already in darkness, but inhibition was significantly increased upon red light exposure. Inhibition may be ascribed to cell cytotoxicity since the short-term incubation would not detect effects on cell proliferation. Similar effects were observed when highly invasive melanoma cells were treated with Ver-MSNs [40]

Since the in vitro experiments showed that Ver-MSNs plus red light has a strong cytotoxic activity, we performed in vivo experiments assessing the antitumor effect of Ver-MSNs combined with light in mice carrying established transplantable melanomas. Results showed that indeed this treatment substantially inhibits the tumor growth compared with control treatments using glycerol or MSNs alone. It is conceivable that mesoporous silica nanoparticles were concentrated into the tumor mass through passive targeting due to leaky blood vessels and poor lymphatic drainage as reported for many types of nanoparticles [41]. The cytotoxic activity of Ver-MSNs may be increased by the ability of mesoporous silica nanoparticles to be internalized into cells mainly through clathrin mediated endocytosis and pinocytosis in the absence of known cell surface receptors [4,42]. The internalization process along with nanoparticles size may account also for

the mild cytotoxic effect shown by the empty MSNs in our in vitro and in vivo experiments [43]. An intriguing finding is that treatment with Ver-MNSs also decreased tumor vascularization, which suggest that the in vivo anti-tumor effect may be mediated not only by direct cytotoxicity on tumor cells but also by inhibition of tumor neo-angiogenesis, which was not detected upon treatment with MSNs alone [1,44,45].

5. Conclusions

To sum up, we evaluated the efficacy of photodynamic therapy with verteporfin-loaded mesoporous silica nanoparticles both *in vitro* and *in vivo* model. Results showed that red light irradiated Ver-MSNs are able to reduce significantly tumour growth and to inhibit tumor angiogenesis.

Therefore, our work suggests that verteporfin mesoporous silica nanoparticles is a potential tool to treat skin melanoma.

The following are the supplementary data related to this article.

Supplementary fig. 1

6. Acknowledgements

Authors thank Dr.Silvia Lombardi, University of Eastern Piedmont, Novara, for the help in the drafting of the paper. Part of this work has been supported by RIVinvernizzimRL16_BCRLrehab17_19 fund (Health Sciences of Department).

7. Conflict of interest

The authors declare they have no conflict of interest.

References

[1] H. Cai, E.-A. Cho, Y. Li, J. Sockler, C.R. Parish, B.H. Chong, J. Edwards, T.J. Dodds,

P.M. Ferguson, J.S. Wilmott, R.A. Scolyer, G.M. Halliday, L.M. Khachigian, Melanoma protective antitumor immunity activated by catalytic DNA., Oncogene. (2018). doi:10.1038/s41388-018-0306-0.

[2] J.B. Jeong, S.C. Hong, J.S. Koo, H.J. Jeong, Induction of Apoptosis and Acetylation of Histone H3 and H4 by Arctigenin in the Human Melanoma Cell Line SK-MEL-28, Food and Nutrition Sciences. 2 (2011) 128–132. doi:10.4236/fns.2011.22018.

[3] C. Luo, C.E.M. Weber, W. Osen, A.-K. Bosserhoff, S.B. Eichmüller, The role of microRNAs in melanoma, European Journal of Cell Biology. 93 (2014) 11–22. doi:10.1016/j.ejcb.2014.02.001.

[4] M. Rizzi, S. Tonello, B.M. Estevão, E. Gianotti, L. Marchese, F. Renò, Verteporfin based silica nanoparticle for in vitro selective inhibition of human highly invasive melanoma cell proliferation., Journal of Photochemistry and Photobiology. B, Biology. 167 (2017) 1–6. doi:10.1016/j.jphotobiol.2016.12.021.

[5] M. Wang, B. Geilich, M. Keidar, T. Webster, Killing malignant melanoma cells with protoporphyrin IX-loaded polymersome-mediated photodynamic therapy and cold atmospheric plasma, International Journal of Nanomedicine. Volume 12 (2017) 4117–4127. doi:10.2147/IJN.S129266.

[6] S.S. Erdem, V.A. Obeidin, T. Yigitbasi, S.S. Tumer, P. Yigit, Verteporfin mediated sequence dependent combination therapy against ovarian cancer cell line, Journal of Photochemistry and Photobiology B: Biology. 183 (2018) 266–274. doi:10.1016/j.jphotobiol.2018.04.039.

[7] C.B. Simone, J.S. Friedberg, E. Glatstein, J.P. Stevenson, D.H. Sterman, S.M. Hahn, K.A. Cengel, Photodynamic therapy for the treatment of non-small cell lung cancer., Journal of Thoracic Disease. 4 (2012) 63–75.

doi:10.3978/j.issn.2072-1439.2011.11.05.

[8] A. Dodds, A. Chia, S. Shumack, Actinic keratosis: rationale and management., Dermatology and Therapy. 4 (2014) 11–31. doi:10.1007/s13555-014-0049-y.

[9] P. Agostinis, K. Berg, K.A. Cengel, T.H. Foster, A.W. Girotti, S.O. Gollnick, S.M. Hahn, M.R. Hamblin, A. Juzeniene, D. Kessel, M. Korbelik, J. Moan, P. Mroz, D. Nowis, J. Piette, B.C. Wilson, J. Golab, Photodynamic therapy of cancer: an update., CA: A Cancer Journal for Clinicians. 61 (2011) 250–81. doi:10.3322/caac.20114.

[10] S. Mallidi, S. Anbil, A.-L. Bulin, G. Obaid, M. Ichikawa, T. Hasan, Beyond the Barriers of Light Penetration: Strategies, Perspectives and Possibilities for Photodynamic Therapy., Theranostics. 6 (2016) 2458–2487. doi:10.7150/thno.16183.

[11] E.B. Turkoglu, R. Pointdujour-Lim, A. Mashayekhi, C.L. Shields, Photodynamic therapy as primary treatment for small choroidal melanoma, Retina. (2018) 1. doi:10.1097/IAE.0000000000002169.

[12] D. van Straten, V. Mashayekhi, H.S. de Bruijn, S. Oliveira, D.J. Robinson, Oncologic Photodynamic Therapy: Basic Principles, Current Clinical Status and Future Directions., Cancers. 9 (2017). doi:10.3390/cancers9020019.

[13] E.K. Konstantinou, S. Notomi, C. Kosmidou, K. Brodowska, A. Al-Moujahed, F. Nicolaou, P. Tsoka, E. Gragoudas, J.W. Miller, L.H. Young, D.G. Vavvas, Verteporfin-induced formation of protein cross-linked oligomers and high molecular weight complexes is mediated by light and leads to cell toxicity, Scientific Reports. 7 (2017) 46581. doi:10.1038/srep46581.

[14] E. Gianotti, B.M. Estevão , I. Miletto, S. Tonello, F. Renò, L. Marchese, Verteporfin based silica nanoplatform for photodynamic therapy, ChemistrySelect. 1 (2016) 127–131. doi:10.1002/slct.201600004.

[15] E. Gianotti, B. Martins Estevão, F. Cucinotta, N. Hioka, M. Rizzi, F. Renò, L. Marchese, An Efficient Rose Bengal Based Nanoplatform for Photodynamic Therapy, Chemistry - A European Journal. 20 (2014) 10921–10925. doi:10.1002/chem.201404296.

[16] Y.-Y. Huang, S.K. Sharma, T. Dai, H. Chung, A. Yaroslavsky, M. Garcia-Diaz, J. Chang, L.Y. Chiang, M.R. Hamblin, Can nanotechnology potentiate photodynamic therapy?, Nanotechnology Reviews. 1 (2012) 111–146. http://www.ncbi.nlm.nih.gov/pubmed/26361572 (accessed July 25, 2018).

[17] S.Bayir, A. Barras, R. Boukherroub, S. Szunerits, L. Raehm, S. Richeter, J.-O. Durand, Mesoporous silica nanoparticles in recent photodynamic therapy applications, Photochemical Photobiological Sciences. 17(2018) 1651-1674. doi:10.1039/c8pp00143j

[18] B.M. Cellamare, P. Fini, A. Agostiano, S. Sortino, P. Cosma, Identification of Ros Produced by Photodynamic Activity of Chlorophyll/Cyclodextrin Inclusion Complexes, Photochemistry and Photobiology. 89 (2013) 432–441. doi:10.1111/j.1751-1097.2012.01238.x.

[19] M. Ginouves, B. Carme, P. Couppie, G. Prevot, Comparison of tetrazolium salt assays for evaluation of drug activity against Leishmania spp., Journal of Clinical Microbiology. 52 (2014) 2131–8. doi:10.1128/JCM.00201-14.

[20] L. Śliwka, K. Wiktorska, P. Suchocki, M. Milczarek, S. Mielczarek, K. Lubelska, T. Cierpiał, P. Łyżwa, P. Kiełbasiński, A. Jaromin, A. Flis, Z. Chilmonczyk, The Comparison of MTT and CVS Assays for the Assessment of Anticancer Agent Interactions., PloS One. 11 (2016) e0155772. doi:10.1371/journal.pone.0155772.

[21] P.D. Ray, B.-W. Huang, Y. Tsuji, Reactive oxygen species (ROS) homeostasis and redox regulation in cellular signaling., Cellular Signalling. 24 (2012) 981–90.

doi:10.1016/j.cellsig.2012.01.008.

[22] M. Broekgaarden, R. Weijer, T.M. van Gulik, M.R. Hamblin, M. Heger, Tumor cell survival pathways activated by photodynamic therapy: a molecular basis for pharmacological inhibition strategies., Cancer Metastasis Reviews. 34 (2015) 643–90. doi:10.1007/s10555-015-9588-7.

[23] B. Martins Estevão, I. Miletto, L. Marchese, E. Gianotti, Optimized Rhodamine B labeled mesoporous silica nanoparticles as fluorescent scaffolds for the immobilization of photosensitizers: a theranostic platform for optical imaging and photodynamic therapy, Physical Chemistry Chemical Physics. 18 (2016) 9042–9052. doi:10.1039/C6CP00906A.

[24] A.P. Gerola, J. Semensato, D.S. Pellosi, V.R. Batistela, B.R. Rabello, N. Hioka, W. Caetano, Chemical determination of singlet oxygen from photosensitizers illuminated with LED: New calculation methodology considering the influence of photobleaching, Journal of Photochemistry and Photobiology A: Chemistry. 232 (2012) 14–21. doi:10.1016/j.jphotochem.2012.01.018.

[25] B.R. Rabello, A.P. Gerola, D.S. Pellosi, A.L. Tessaro, J.L. Aparício, W. Caetano, N. Hioka, Singlet oxygen dosimetry using uric acid as a chemical probe: Systematic evaluation, Journal of Photochemistry and Photobiology A: Chemistry. 238 (2012) 53–62. doi:10.1016/j.jphotochem.2012.04.012.

[26] J. Zhan, Z. Ma, D. Wang, X. Li, X. Li, L. Le, A. Kang, P. Hu, L. She, F. Yang, Magnetic and pH dual-responsive mesoporous silica nanocomposites for effective and low-toxic photodynamic therapy., International Journal of Nanomedicine. 12 (2017) 2733–2748. doi:10.2147/IJN.S127528.

[27] D. Wang, C.R. Stockard, L. Harkins, P. Lott, C. Salih, K. Yuan, D. Buchsbaum, A. Hashim, M. Zayzafoon, R.W. Hardy, O. Hameed, W. Grizzle, G.P. Siegal, Immunohistochemistry in the evaluation of neovascularization in tumor

xenografts., Biotechnic & Histochemistry : Official Publication of the Biological Stain Commission. 83 (2008) 179–89. doi:10.1080/10520290802451085.

[28] N.H. Matthews, W.-Q. Li, A.A. Qureshi, M.A. Weinstock, E. Cho, Epidemiology of Melanoma, Codon Publications, 2017. doi:10.15586/CODON.CUTANEOUSMELANOMA.2017.CH1.

[29] E.P. Markova-Car, D. Jurišić, N. Ilić, S. Kraljević Pavelić, Running for time: circadian rhythms and melanoma, Tumor Biology. 35 (2014) 8359–8368. doi:10.1007/s13277-014-1904-2.

[30] M.K. Tripp, M. Watson, S.J. Balk, S.M. Swetter, J.E. Gershenwald, State of the science on prevention and screening to reduce melanoma incidence and mortality: The time is now, CA: A Cancer Journal for Clinicians. 66 (2016) 460–480. doi:10.3322/caac.21352.

[31] R.L. Siegel, K.D. Miller, A. Jemal, Cancer statistics, 2016, CA: A Cancer Journal for Clinicians. 66 (2016) 7–30. doi:10.3322/caac.21332.

[32] M.S. Soengas, S.W. Lowe, Apoptosis and melanoma chemoresistance, Oncogene. 22 (2003) 3138–3151. doi:10.1038/sj.onc.1206454.

[33] V. Monge-Fuentes, L.A. Muehlmann, R.B. de Azevedo, Perspectives on the application of nanotechnology in photodynamic therapy for the treatment of melanoma, Nano Reviews. 5 (2014) 24381. doi:10.3402/nano.v5.24381.

[34] A.A. Sebak, I.E.O. Gomaa, A.N. ElMeshad, M.H. AbdelKader, Targeted photodynamic-induced singlet oxygen production by peptide-conjugated biodegradable nanoparticles for treatment of skin melanoma, Photodiagnosis and Photodynamic Therapy. 23 (2018) 181–189. doi:10.1016/j.pdpdt.2018.05.017.

[35] E. V. Maytin, S. Anand, M. Riha, S. Lohser, A. Tellez, R. Ishak, L. Karpinski, J. Sot,

B. Hu, A. Denisyuk, S.C. Davis, A. Kyei, A. Vidimos, 5-Fluorouracil Enhances Protoporphyrin IX Accumulation and Lesion Clearance during Photodynamic Therapy of Actinic Keratoses: A Mechanism-Based Clinical Trial, Clinical Cancer Research. 24 (2018) 3026–3035. doi:10.1158/1078-0432.CCR-17-2020.

[36] E. Debefve, B. Pegaz, H. van den Bergh, G. Wagnières, N. Lange, J.-P. Ballini, Video monitoring of neovessel occlusion induced by photodynamic therapy with verteporfin (Visudyne), in the CAM model., Angiogenesis. 11 (2008) 235–43. doi:10.1007/s10456-008-9106-4.

[37] P. Mroz, A. Yaroslavsky, G.B. Kharkwal, M.R. Hamblin, Cell death pathways in photodynamic therapy of cancer., Cancers. 3 (2011) 2516–39. doi:10.3390/cancers3022516.

[38] A.P. Castano, T.N. Demidova, M.R. Hamblin, Mechanisms in photodynamic therapy: part two-cellular signaling, cell metabolism and modes of cell death., Photodiagnosis and Photodynamic Therapy. 2 (2005) 1–23. doi:10.1016/S1572-1000(05)00030-X.

[39] K. Ichikawa, Y. Takeuchi, S. Yonezawa, T. Hikita, K. Kurohane, Y. Namba, N. Oku, Antiangiogenic photodynamic therapy (PDT) using Visudyne causes effective suppression of tumor growth, Cancer Letters. 205 (2004) 39–48. doi:10.1016/j.canlet.2003.10.001.

[40] M. Rizzi, S. Tonello, B.M. Estevão, E. Gianotti, L. Marchese, F. Renò, Verteporfin based silica nanoparticle for in vitro selective inhibition of human highly invasive melanoma cell proliferation, Journal Photochem Photobiol B. 167 (2017)1-6. doi: 10.1016/j.jphotobiol.2016.12.021.

[41] I. Helfrich, D. Schadendorf, Blood vessel maturation, vascular phenotype and angiogenic potential in malignant melanoma: one step forward for overcoming anti-angiogenic drug resistance?, Molecular Oncology. 5 (2011) 137–49.

doi:10.1016/j.molonc.2011.01.003.

[42] I. Slowing, J. Viveroescoto, C. Wu, V. Lin, Mesoporous silica nanoparticles as controlled release drug delivery and gene transfection carriers ☆, Advanced Drug Delivery Reviews. 60 (2008) 1278–1288. doi:10.1016/j.addr.2008.03.012.

[43] I.-Y. Kim, E. Joachim, H. Choi, K. Kim, Toxicity of silica nanoparticles depends on size, dose, and cell type. Nanomedicine. 11 (2015) 1407-16. doi: 10.1016/j.nano.2015.03.004.

[44] S. Park, C.M. Sorenson, N. Sheibani, PECAM-1 isoforms, eNOS and endoglin axis in regulation of angiogenesis., Clinical Science (London, England : 1979). 129 (2015) 217–34. doi:10.1042/CS20140714.

[45] H.M. Delisser, M. Christofidou-Solomidou, R.M. Strieter, M.D. Burdick, C.S. Robinson, R.S. Wexler, J.S. Kerr, C. Garlanda, J.R. Merwin, J.A. Madri,'w, S.M. Albelda, M.N. Milano, Involvement of Endothelial PECAM-1/CD31 in Angiogenesis, 1997. https://www.ncbi.nlm.nih.gov/pmc/articles/PMC1857836/pdf/amjpathol00021-0033.pdf (accessed July 25, 2018).

Figure 1 Preparation of nanoparticles.

Schematic representation of the procedure used to obtain Verteporfin-functionalized Mesoporous silica nanoparticles.

Figure 2 FTIR spectra of MSNs (black curve) and Ver-MSNs (green curve) in the high (section A) and low (section B) frequency region.

Figure 3 Production of singlet oxygen.

Decay curves of the UA absorption band at 292 nm as a function of the irradiation time in the presence of NH2-MSNs (empty circles) and Ver-MSNs (full black circles).

Figure 4 Effect of Verteporfin-mesoporous silica nanoparticles on B16F10 cells in dark conditions and under red light exposure.

MTT assay of B16F10 cells was carried out after 4 hours incubations with MSNs loaded with Verteporfin. Cellular toxicity was increased in red light irradiated Ver-MSNs.

Results are expressed as mean values ± standard deviation.

***p<0.001 referred to non-irradiated (0 seconds) plain mesoporous silica nanoparticles MSNs.

°°°p<0.001 referred to irradiated mesoporous silica nanoparticles MSNs.

^p<0.05, ^^p<0.01, ^^^p<0.001 compared cell viability between dark Ver-MSNs and shielded Ver-MSNs.

Figure 5a Effects of Verteporfin-loaded mesoporous silica nanoparticles on melanoma growth (B16F10) when mice are exposed to red light.

Results are expressed as mean values ± standard deviation.

*p<0.05, ***p<0.001 referred to the control (vehicle)

b Ver-MSNs inhibit mouse melanoma tumor growth

Results are expressed as mean values ± standard deviation.

***p<0.001 referred to the control

°p<0.05 referred to MSNs

c Representative photos of tumor masses obtained after sacrifice of animals treated with glycerol (Vehicle), MSNs and Ver-MSNs.

Figure 6a Immunofluorescent images of CD31 staining (green) as an indication of tumor angiogenesis and nuclear DAPI counterstain (blue). Magnification=20X

b Green fluorescence quantification.

*p<0.05, ***p<0.001 referred to the vehicle = control

°p<0.05 referred to MSNs

Highlights

- Melanoma is one of the most lethal tumors among the skin cancers.
- Verteporfin (Ver), a second-generation photosensitizer, has been conjugated with mesoporous silica nanoparticles (MSNs)
- In vitro Ver-MSNs (0.1-10 microg/ml) stimulated by red light (693nm) inhibit B16F10 mouse melanoma cells growth
- In vivo topically administrated Ver-MSNs (5 microg/ml) reduced melanoma tumor mass and vascularization in mice.
- PTD using Ver-MSNs could be a new promising approach for melanoma treatment.

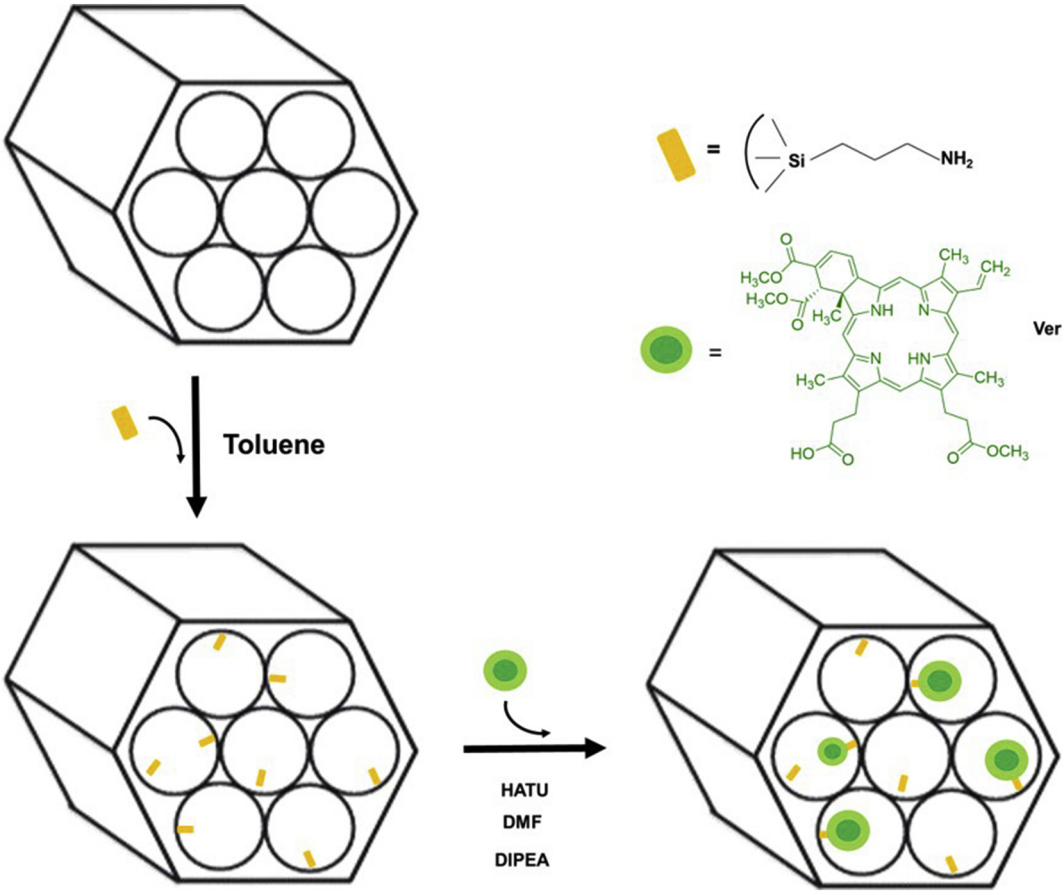

Figure 1

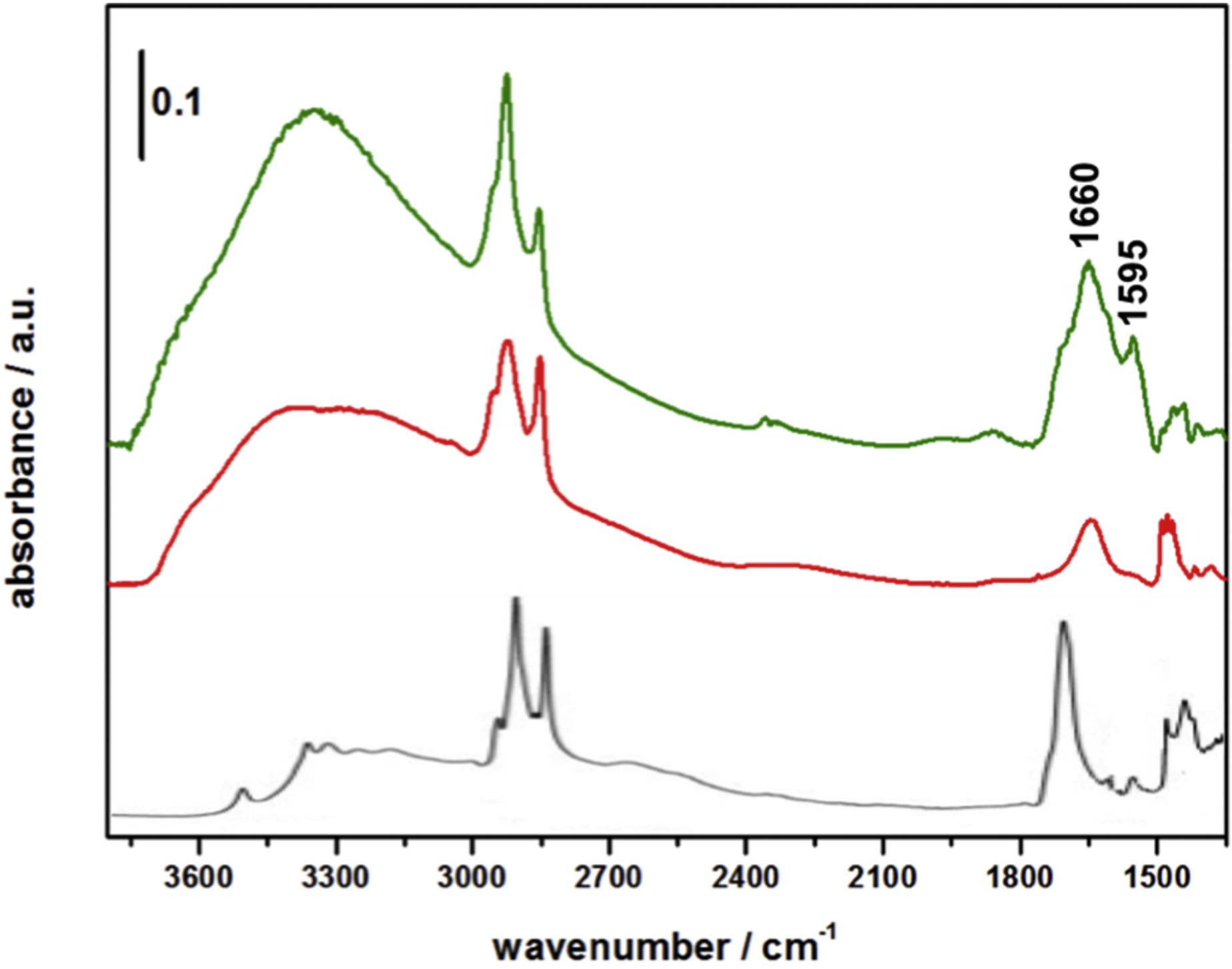
0.1
1660
1595
absorbance / a.u.
3600
3300
3000
2700
2400
2100
1800
1500
wavenumber / cm-1

Figure 2

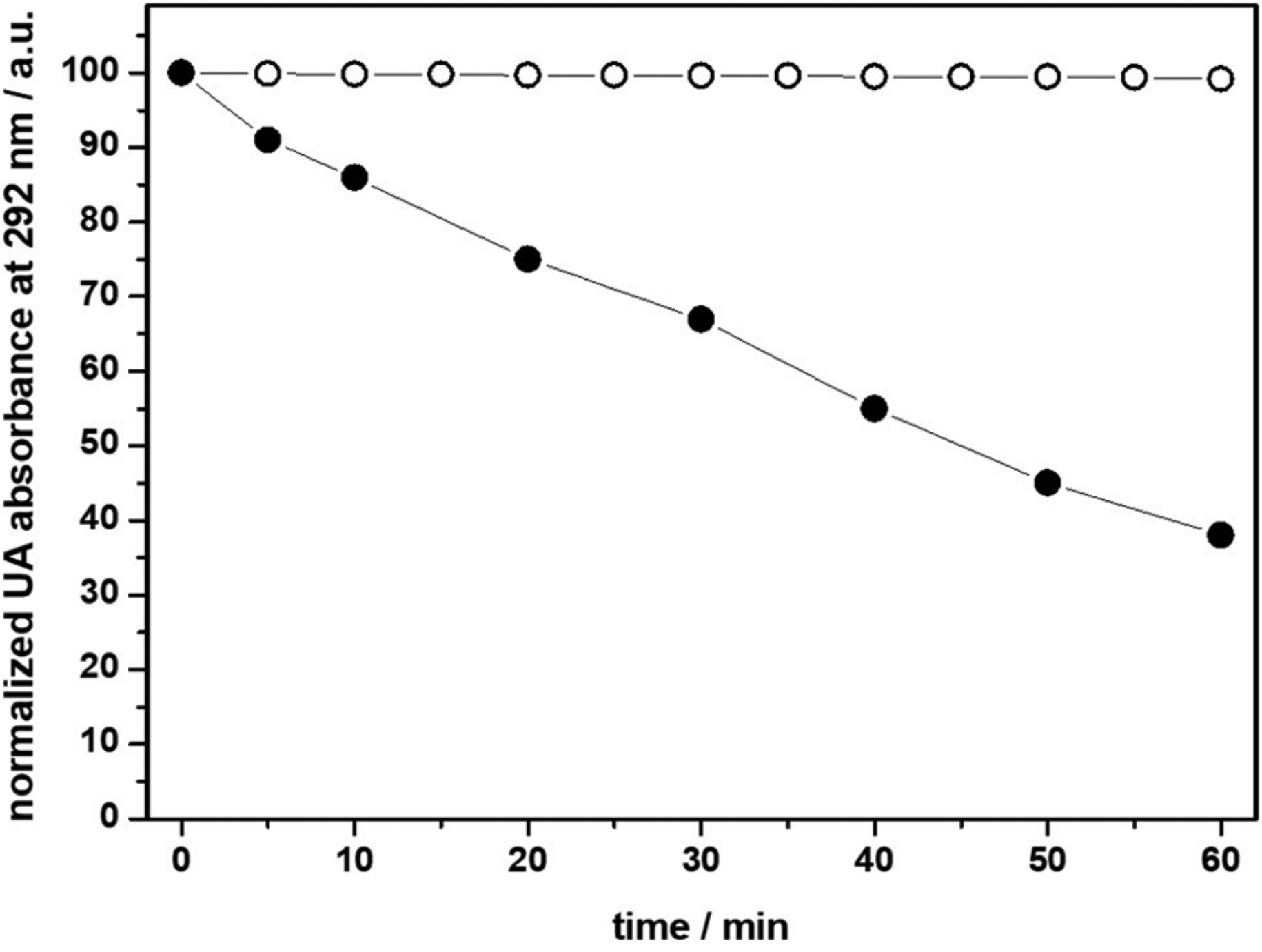
normalized UA absorbance at 292 nm / a.u.
100
90
80
70
60
50
40
30
20
10
0
0
10
20
30
40
50
60
time / min

Figure 3

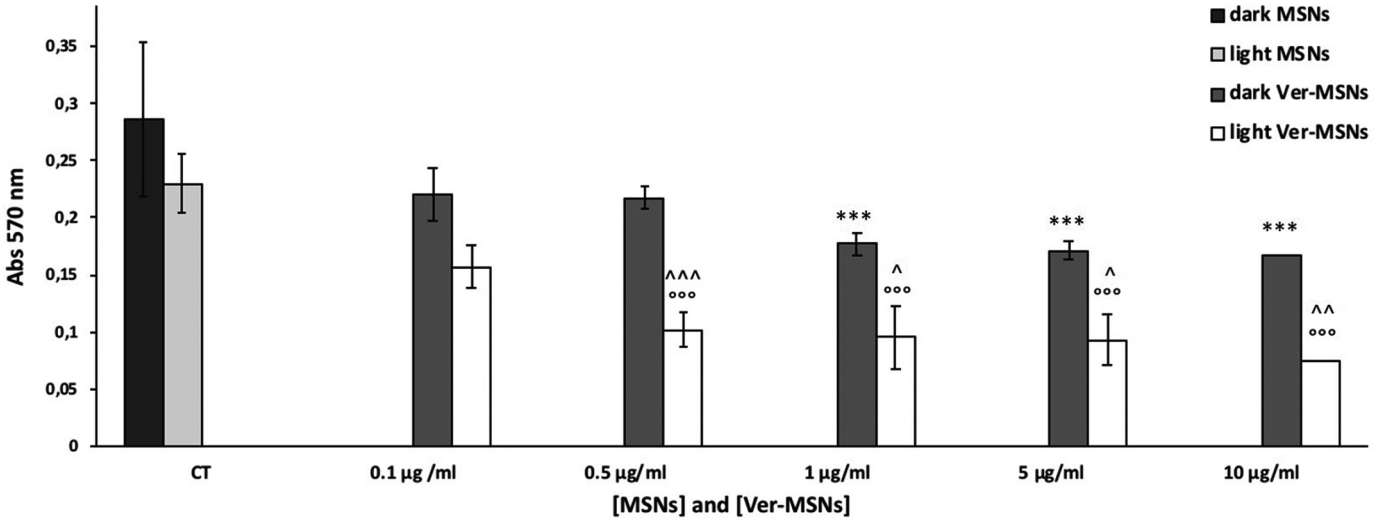
dark MSNs
light MSNs
dark Ver-MSNs
light Ver-MSNs
Abs 570 nm
0,35
0,3
0,25
0,2
0,15
0,1
0,05
0
***
***
***
^^^
°°°
^
°°°
^
°°°
^^
°°°
CT
0.1 µg /ml
0.5 µg/ml
1 µg/ml
5 µg/ml
10 µg/ml
[MSNs] and [Ver-MSNs]

Figure 4

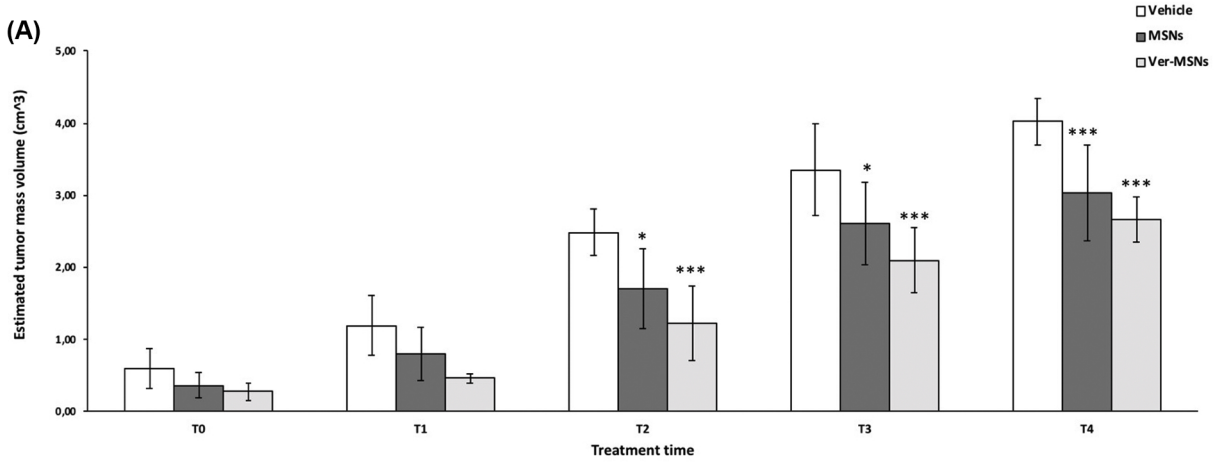
(A)
Vehicle
MSNs
Ver-MSNs
Estimated tumor mass volume (cm^3)
5,00
4,00
3,00
2,00
1,00
0,00
*
***
*
***
***
***
T0
T1
T2
T3
T4
Treatment time

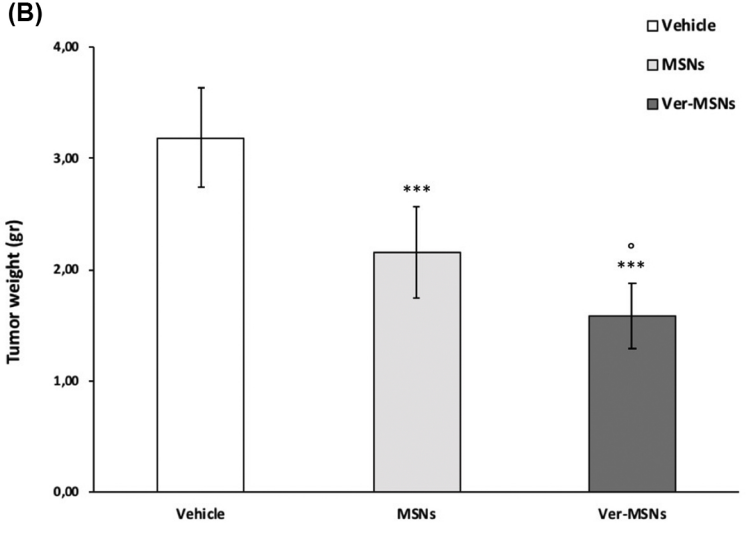
(B)
Vehicle
MSNs
Ver-MSNs
Tumor weight (gr)
4,00
3,00
2,00
1,00
0,00
***
°
***
Vehicle
MSNs
Ver-MSNs

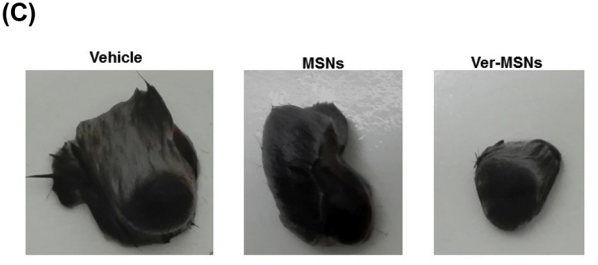
(C)
Vehicle
MSNs
Ver-MSNs

Figure 5

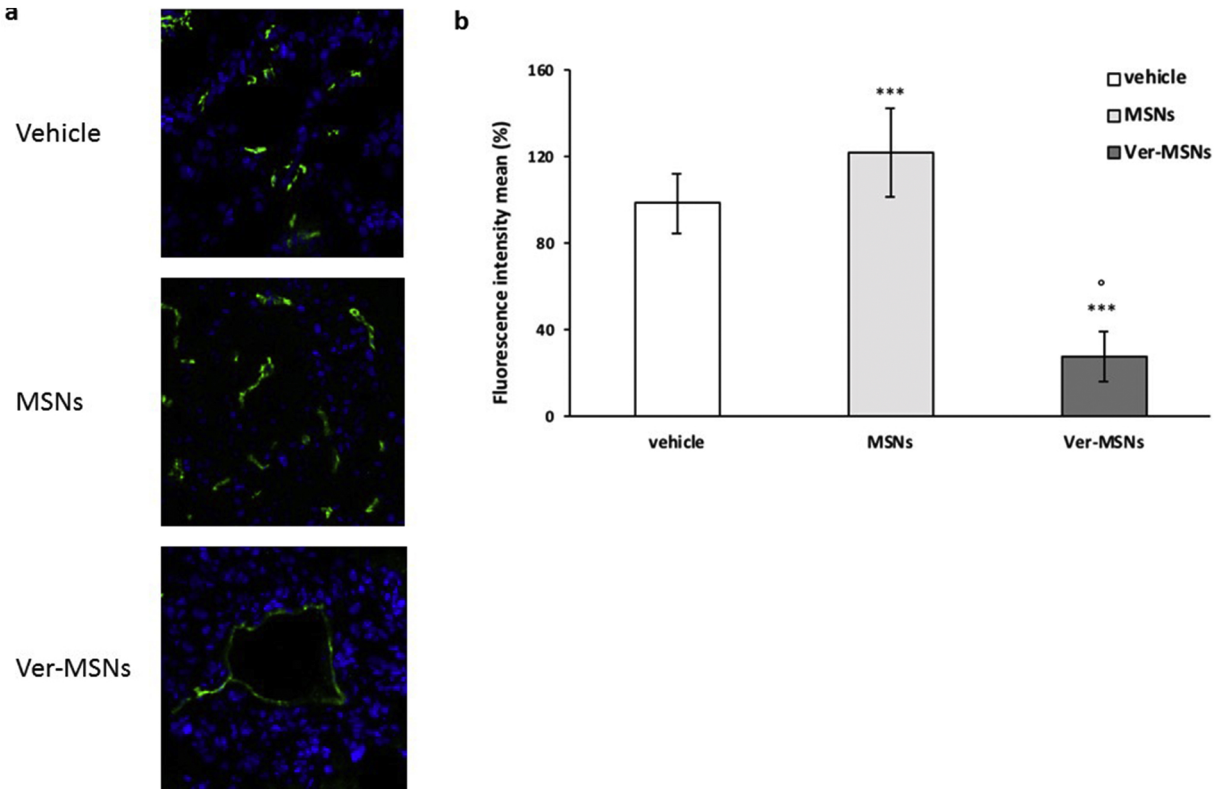
a
Vehicle
MSNs
Ver-MSNs
b
Fluorescence intensity mean (%)
160
120
80
40
0
***
***
°
vehicle
MSNs
Ver-MSNs
vehicle
MSNs
Ver-MSNs

Figure 6

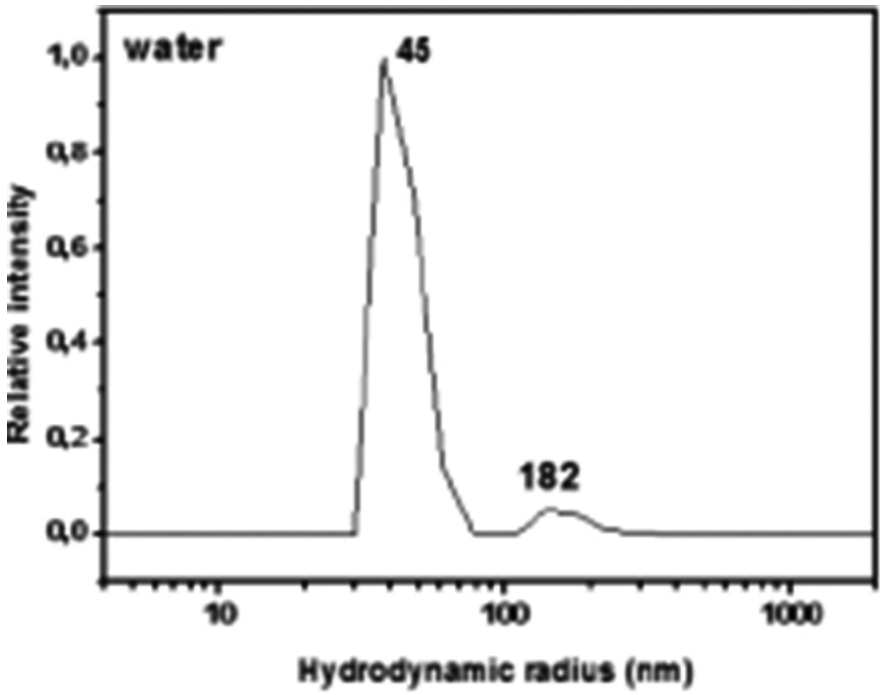
water
45
182
Relative intensity
1,0
0,8
0,6
0,4
0,2
0,0
10
100
1000
Hydrodynamic radius (nm)

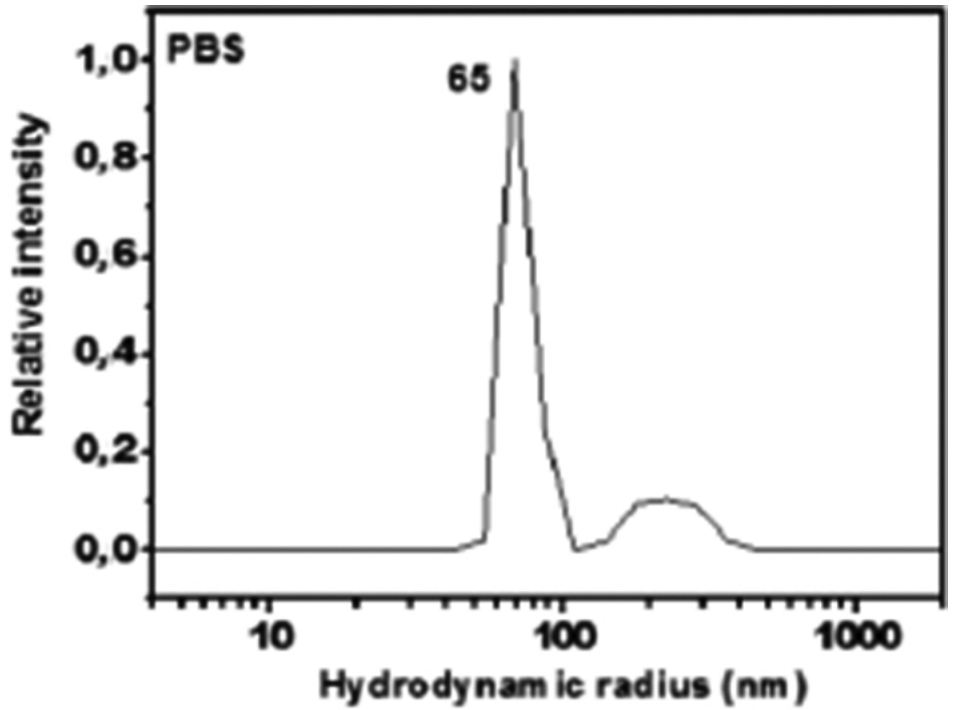
PBS
65
Relative intensity
1,0
0,8
0,6
0,4
0,2
0,0
10
100
1000
Hydrodynamic radius (nm)

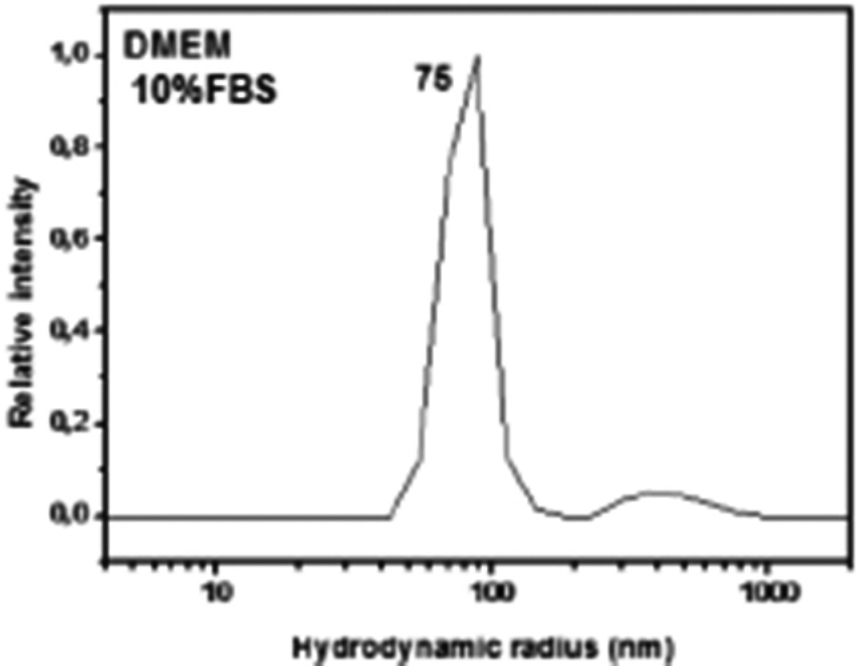
DMEM
10%FBS
75
Relative intensity
1,0
0,8
0,6
0,4
0,2
0,0
10
100
1000
Hydrodynamic radius (nm)

Figure 7